



UDC 621.315.592+538.9

<https://www.doi.org/10.33910/2687-153X-2021-2-4-165-171>

## The valence zone structure in $\text{PbSb}_2\text{Te}_4$ and anisotropy of hole relaxation time

S. A. Nemov<sup>✉1</sup>, V. D. Andreeva<sup>1</sup>, V. Volkhin<sup>2</sup>, V. Yu. Proklova<sup>3</sup>, Yu. V. Ulashkevich<sup>4</sup>

<sup>1</sup> Peter the Great St. Petersburg Polytechnic University, 29 Polytechnicheskaya Str., Saint Petersburg 195251, Russia

<sup>2</sup> Saint Petersburg Electrotechnical University "LETI", 5 Professora Popova Str., Saint Petersburg 197376, Russia

<sup>3</sup> Transbaikal State University, 30 Aleksandro-Zavodskaya Str., Chita 672039, Russia

<sup>4</sup> Ioffe Institute, 26 Polytechnicheskaya Str., Saint Petersburg 194021, Russia

### Authors

Sergey A. Nemov, ORCID: 0000-0001-7673-6899, e-mail: [nemov\\_s@mail.ru](mailto:nemov_s@mail.ru)

Valentina D. Andreeva, ORCID: 0000-0001-6085-4153, e-mail: [avd2007@bk.ru](mailto:avd2007@bk.ru)

Vitaliy Volkhin, e-mail: [vitaly10121998@gmail.com](mailto:vitaly10121998@gmail.com)

Viktoriya Yu. Proklova, e-mail: [PVictoria78@mail.ru](mailto:PVictoria78@mail.ru)

Yuri V. Ulashkevich

**For citation:** Nemov, S. A., Andreeva, V. D., Volkhin, V., Proklova, V. Yu., Ulashkevich, Yu. V. (2021) The valence zone structure in  $\text{PbSb}_2\text{Te}_4$  and anisotropy of hole relaxation time. *Physics of Complex Systems*, 2 (4), 165–171.

<https://www.doi.org/10.33910/2687-153X-2021-2-4-165-171>

**Received** 7 September 2021; reviewed 21 September 2021; accepted 21 September 2021.

**Funding:** The study did not receive any external funding.

**Copyright:** © S. A. Nemov, V. D. Andreeva, V. Volkhin, V. Yu. Proklova, Yu. V. Ulashkevich (2021). Published by Herzen State Pedagogical University of Russia. Open access under [CC BY-NC License 4.0](https://creativecommons.org/licenses/by-nc/4.0/).

**Abstract.** The article analyses the existing set of data on the temperature dependences of the main kinetic coefficients and the IR-reflection spectra  $R(\nu)$  of the  $\text{PbSb}_2\text{Te}_4$  crystals. The form of the Fermi surface is discussed. The anisotropy of holes' effective mass and relaxation time is estimated. The complex structure of the valence zone is confirmed, the values of these parameters are refined.

Complex X-ray studies of the structure and composition of  $\text{PbSb}_2\text{Te}_4$  samples gave the possibilities to clarify the real crystal structure and explain the number of features in the IR-reflection spectra.

**Keywords:** crystal  $\text{PbSb}_2\text{Te}_4$ , semiconductor, transport properties, temperature, band structure, Fermi surface, IR-reflection, X-ray investigations.

### Introduction

$\text{PbSb}_2\text{Te}_4$  crystals belong to the class of layered tetradymite-like chalcogenides having a rhombohedral symmetry. The typical examples of this class are well-studied thermoelectric materials: bismuth ( $\text{Bi}_2\text{Te}_3$ ) and antimony ( $\text{Sb}_2\text{Te}_3$ ) tellurids (Goltsman et al. 1972).

$\text{PbSb}_2\text{Te}_4$  crystals usually grow with a significant deviation from the stoichiometric composition. The main feature of the samples is a large number of different electrically active point defects leading to the hole conductivity (Shelimova et al. 2004; 2007). Most of the studied crystals according to the data from the Hall effect have high concentrations of holes  $p \sim 1 \times 10^{20} \text{ cm}^{-3}$  (Zhitinskaya et al. 2008).

The strong anisotropy of the crystal lattice determines the anisotropy in the physical properties that are described by the tensors. In particular, the electrical conductivity and the Seebeck effect are described by the second rank tensors  $\sigma_{ik}$  and  $S_{ik}$ , respectively, which have two independent components along the inversion-rotary axis 3 ( $\sigma_{33}$  and  $S_{33}$ ) and in the plane cleavage of crystals ( $\sigma_{11}$  and  $S_{11}$ ). The Hall and Nernst-Ettingshausen effects are characterized by the third rank tensors ( $R_{ikl}$  and  $Q_{ikl}$  coefficients, respectively).

In (Nemov et al. 2013; 2014; Shelimova et al. 2007; Zhitinskaya et al. 2008), the electrophysical properties of  $\text{PbSb}_2\text{Te}_4$  crystals were studied.  $\text{PbSb}_2\text{Te}_4$  optical properties were not studied well. Only reflection spectra were measured (Nemov et al. 2016) and their anisotropy (Nemov et al. 2020).

The greatest anisotropy of the electrophysical properties of  $PbSb_2Te_4$  crystals detected among the layered thermoelectricity of the anisotropy of  $PbSb_2Te_4$  crystals (lead-antimony telluride) (Shelimova et al. 2007) is very interesting for the scientific research and from the point of view of the possible practical applications. In particular, the crystals have a significant anisotropy of the thermopower coefficients  $\Delta S = S_{33} - S_{11}$  reaching  $75 \mu V/K$  at room temperature.

## Crystals

The studied  $PbSb_2Te_4$  crystals were synthesized at the Baikov Institute of Metallurgy and Material Science, Russian Academy of Sciences. Their physical, chemical and electrophysical properties were studied in (Shelimova et al. 2004; 2007).

The  $PbSb_2Te_4$  crystal lattice has rhombohedral symmetry. The crystals have a layered structure, which is based on the seven-layer packets of the atomic planes  $TeSbTePbTeSbTe$ . Those packets orderly alternate in the direction of the inversion-rotary axis of the third order  $\bar{3}$ .

Usually, the hexagonal elementary cell, containing 3 seven-layer packages is used. It has the following parameters:  $a = 0.4350$  nm and  $c = 4.1712$  nm, spatial symmetry  $R\bar{3}m$  (Shelimova et al. 2004; 2007).

The chemical bond between atoms inside the seven-layer packages is ion-covalent, and between the edge tellurium atoms (Te-Te)—weak van der Waals forces.

We studied 4  $PbSb_2Te_4$  monocrystals with rather large geometric dimensions of  $4 \times 4 \times 20$  mm, including along the  $\bar{3}$  axis.

Radiographs were got with the help of Bruker D8 Advance diffractometer, in monochromated  $Cu_{K\alpha}$  - radiation at the bundle width of 15 mm, with the divergence of 1 degree, which ensured a wide coverage of the surface.

We studied  $PbSb_2Te_4$  samples in the direction of the inversion-rotary axis corresponding to the perpendicular direction of the cleavage plane in the monocrystal, and  $PbSb_2Te_4$  and  $PbSb_2Te_4:Cu$  doped with copper (up to 0.1%) in the direction of the cleavage plane.

All studied crystals have the rhombohedral symmetry and structural parameters close to their values in (Shelimova et al. 2004; 2007). However, our results suggest that in  $PbSb_2Te_4$  crystals there are two structures close in parameters with the symmetry  $R\bar{3}m$  and  $R32$ , and  $R\bar{3}m$  phase dominates. Figure 1 shows our results.

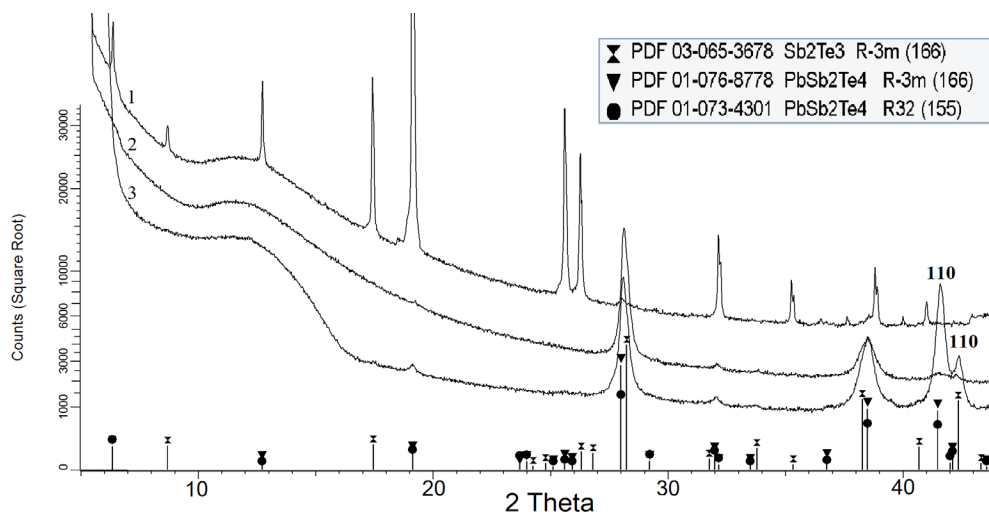


Fig. 1. Radiographs of the  $PbSb_2Te_4:Cu$  sample from the chip surface (1); the same (2) and the sample without copper (3) in the perpendicular  $C3$  axis direction

The strong effect of preferential orientation of crystals in the direction 001 plane of the cleavage is visible on radiographs.

According to the calculation by Rietveld, it has been found that the content of the phase  $R32$  with the lattice parameters  $a = 0.435$  nm,  $c = 4.171$  nm does not exceed 2.5–3 wt.% in samples with Cu, and less

than 1% in the sample without Cu. The amount of  $\text{Sb}_2\text{Te}_3$  with the structure  $R\bar{3}m$  in all the samples is at the level of several percent. Copper atoms having minimal dimensions (0.071 nm against 0.090 nm for Pb and Sb, and 0.111 nm for Te) during the doping of the monocrystal are embedded in the form of ions mostly between the cleavage planes. This leads to local microdeformations of the crystal lattice  $R\bar{3}m$  in the perpendicular direction to the trigonal axis  $C_3$ , as evidenced by significant, up to almost complete disappearance on the radiograph, broadening lines 110 (curves 2 and 3,  $2\Theta = 40-43^\circ$ , Fig. 1). Relative microdeformations in these directions are 0.27% and 0.35% in five-layer  $\text{Sb}_2\text{Te}_3$  and seven-layer  $\text{PbSb}_2\text{Te}_4$  structures, respectively. The ratio  $c/a$  decreases from 7.15 to 7.12 for  $\text{Sb}_2\text{Te}_3$  and from 9.62 to 9.57 for  $\text{PbSb}_2\text{Te}_4$ , which also indicates a less strong effect of copper atoms to change the parameter  $c$  than  $a$  (the introduction of Cu atoms into interlayer spaces of singlets has a relatively smaller effect on the dimensional characteristics of the crystalline cell than their location in more packed planes perpendicular to the  $C_3$  axes).

### Energy spectrum of holes

This section summarizes the results of transfer phenomena studies (Nemov et al. 2013; 2014; Shelimova et al. 2007; Zhitinskaya et al. 2008); the energy spectrum of holes and the parameters of current carriers are clarified.

Additional measurements of the kinetic coefficients on  $\text{PbSb}_2\text{Te}_4$  crystals with the same composition as in the works (Nemov et al. 2013; 2014; Shelimova et al. 2004; 2007; Zhitinskaya et al. 2008) showed that they have similar magnitudes and temperature dependencies. So, let us go directly to the discussion of the results.

In the works (Nemov et al. 2013; 2014; Shelimova et al. 2007; Zhitinskaya et al. 2008), the valence zone structure of  $\text{PbSb}_2\text{Te}_4$  and the scattering mechanisms were studied by measuring the temperature dependences of four kinetic coefficients: electrical conductivity ( $\sigma$ ), Hall coefficients ( $R$ ), thermopower ( $S$ ) and transverse effect of Firstly, at the temperatures  $T = 120$  K from 4 kinetic coefficients, the  $r_{kk}$  scattering parameter was determined in the  $k$  direction with the help of the formula:

$$\frac{Q_{ikl}}{R_{ikl}\sigma_{kk}S_{kk}} = \frac{r_{kk} - 0.5}{r_{kk} + 1},$$

where indices  $i, k, l$  denote the direction of measuring the electric field (EMF)  $E_i$ , Hall and Nernst-Ettingshausen effects ( $i$ ),  $k$ -components of the current density  $j_k$  and the temperature gradient  $\frac{\partial T}{\partial X_k}$ ,  $l$  is  $H_l$  component of the external magnetic field.

Further, from the data on the thermopower coefficient of  $S_{kk}$  with the known  $r_{kk}$ , it is possible to determine the reduced chemical potential  $\mu^* = \frac{\mu}{k_0 T}$ :

$$S_{kk}^{(T)} = \frac{k_0}{e} \frac{\pi^2}{3} \frac{k_0 T}{\mu(T)} (r_{kk} + 1), \quad (1)$$

where:  $k_0$  is the Boltzmann constant,  $e$  is an electron charge module.

(Q) their anisotropy in temperature range 77–450 K.

Holes' concentration ( $p$ ) in the studied crystals was determined from the greater component of Hall Tensor  $R_{123}$  at the temperature of 77 K, as adopted in the study of layered anisotropic materials properties of  $A_2^V B_3^V$  (type  $\text{Bi}_2\text{Te}_3$ ) (Golzman et al. 1972).

In  $\text{PbSb}_2\text{Te}_4$  crystals, there is a number of features in the temperature dependences of the kinetic coefficients, in particular, both components of Hall Tensor  $R_{123}$  and  $R_{321}$  are characterized by the constant growth by 1.5–2 times at the range of 77–300 K. The ratio of the thermopower coefficient ( $S$ ) to the temperature  $\frac{S}{T}(T)$  strongly depends on the temperature, which should be approximately constant at the temperature range 77–450 in one zone model (Nemov et al. 2013).

So, the results of the transfer phenomena indicate the complexity of the zone structure scattering  $\text{PbSb}_2\text{Te}_4$  and participating in transfer phenomena several types of charge carriers.

It should be noted that the analysis of experimental data was difficult because of almost the same high concentration of holes  $\rho \approx 3.2 \times 10^{20} \text{ cm}^{-3}$ . Doping with a donor copper admixture (Shelimova et al. 2004; 2007) made it possible to reduce the concentration of holes by about 2 times to  $\rho \approx 3.2 \times 10^{10} \text{ cm}^{-3}$  at the temperatures near the liquid nitrogen temperature 77 K. Kinetic coefficients for this crystal qualitatively and quantitatively can be described in the framework of the one zone model (one variety of current carriers and a quadratic dispersion law). This circumstance, taking into account the strong degeneration of the hole gas, made it possible to determine the parameters of zone spectrum of holes in  $PbSb_2Te_4$  sample with the minimum concentration of holes.

Estimates of the parameters of the zone spectrum were carried out as follows.

Firstly, at the temperatures  $T = 120 \text{ K}$  from 4 kinetic coefficients, the  $r_{kk}$  scattering parameter was determined in the  $k$  direction with the help of the formula:

$$\frac{Q_{ikl}}{R_{ikl}\sigma_{kk}S_{kk}} = \frac{r_{kk} - 0.5}{r_{kk} + 1},$$

where indices  $i, k, l$  are denoted the direction of measuring the electric field (EMF)  $E_i$ , Hall and Nernst-Ettingshausen effects ( $i$ ),  $k$ -components of the current density  $j_k$  and the temperature gradient  $\frac{\partial T}{\partial X_k}$ ,  $l$  is  $H_l$  component of the external magnetic field.

Further, from the data on the thermopower coefficient of  $S_{kk}$  with the known  $r_{kk}$ , it is possible to determine the reduced chemical potential  $\mu^* = \frac{\mu}{k_0T}$ :

$$S_{kk}^{(T)} = \frac{k_0}{e} \frac{\pi^2}{3} \frac{k_0T}{\mu(T)} (r_{kk} + 1), \quad (2)$$

where  $k_0$  is the Boltzmann constant and  $e$  is an electron charge module.

Knowing the value of  $\mu^*(T)$  and using the formula

$$\mu(T) = \mu_0 \left[ 1 - \frac{\pi^2}{12} \left( \frac{k_0T}{\mu} \right)^2 \right], \quad (3)$$

where  $\mu_0 = (0 \text{ K})$ , Fermi level  $E_F$  equal from the determination to the chemical potential at zero temperature  $E_F = \mu_0$  was determined. It turned out to be 0.23 eV.

Then, from the formula for holes concentration

$$p = \frac{8\pi}{3h^3} (2m_d)^{3/2} \mu_0^{3/2}$$

the effective mass of the holes state density  $m_d \approx 0.5 m_0$  ( $m_0$  is a mass of free electron) was determined.

At higher temperatures, Hall coefficient grows noticeably. In semiconductor physics this growth is traditionally associated with the redistribution of current carriers between non-equivalent extremums. So, calculations in this temperature area must be carried out with at least two varieties of free charge carriers, i. e., within a two-zone model.

Preliminary calculations in this model were performed in our work (Nemov et al. 2013), in which the calculation procedure was described in detail. In this work, numerical calculations have been performed within the system of equations for 4 coefficients ( $R, S, \sigma, Q$ ) in a two-zone model. The following values of the model parameters were obtained:

The ratio of mobility of light and heavy holes  $b \approx 4-6$ , the effective mass of  $m_{d_2} \approx 1 m_0$ , the energy gap between zones  $\Delta E_v$  with increasing temperature decreases from the value of  $\Delta E_v \approx 0.24 \text{ eV}$  (at  $T \rightarrow 0 \text{ K}$ ) with the approximate speed  $\frac{d\Delta E_v}{dT} \approx -1 \times 10^{-4} \text{ eV/K}$ .

The qualitative nature of changing the  $PbSb_2Te_4$  zone structure with temperature is shown in Fig. 2. It should be noted that the nature of the evaluations of heavy holes parameters is approximate because of the large number of unknown model parameters.

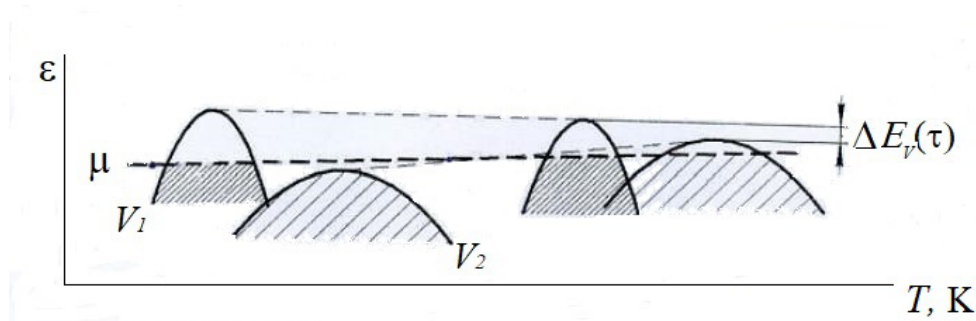


Fig. 2. Temperature displacement of zones  $V_1$ ,  $V_2$  and chemical potential  $\mu$

### Fermi surface

To estimate effective mass anisotropy, it is necessary to know the type of Fermi surface.

Because of the lack of information in the scientific literature about the form of Fermi surface in  $p$ -PbSb<sub>2</sub>Te<sub>4</sub> and extremum place in the Brillouin zone, let us suppose that the maximum in the valence zone is in the center, i. e., in G-point.

As the crystal lattice has symmetry on Neiman principle, Fermi surface should be the ellipsoid of rotation with the rotational axis going parallel to the symmetry axis  $\bar{3}$ , and effective mass tensor will have two components: longitudinal  $m_l$  (oriented along the symmetry axis) and transverse  $m_t$  (perpendicular to  $\bar{3}$ ).

Apparently, the ellipsoids are elongated,  $m_e > m_t$ , since the longitudinal component of the thermopower  $S_e$  (along the  $C_3$  axis) is larger than the transverse component  $S_t$  in the plane cleavage, perpendicular to  $C_3$ . In this case, effective mass anisotropy can be characterized by the parameter  $R\bar{3}m$ .

It should be noted that more complex types of Fermi surface are also possible—two ellipsoids on the symmetry axis  $\bar{3}$ , located symmetrically relative to G-point, as well as the combination of ellipsoids, symmetrically located relative to the axis  $\bar{3}$ .

Unfortunately, from the available data about kinetic coefficients ( $R$ ,  $S$ ,  $\sigma$ ,  $Q$ ) there is no possibility to determine effective mass components  $m_i^*$ , in particular from the electrical conductivity coefficient, since the formula includes the ratio of time relaxation to efficient mass:

$$\sigma = \frac{e^2 n \tau}{m^*}.$$

### Evaluation of effective mass anisotropy and relaxation time of holes

Taking into account the strong anisotropy of PbSb<sub>2</sub>Te<sub>4</sub> physical properties, and also observing the significant anisotropy of the thermopower, it gives us a possibility to suggest the presence of the hole scattering anisotropy. In this case, the relaxation time will be described by the second rank tensor  $\tau_{ik}$ .

In the case when both tensors of the effective mass  $m_{ik}$  and relaxation time  $\tau_{ik}$  are diagonal in the same coordinate axes, the relaxation time will have two independent components—the longitudinal  $\tau_l$  and  $\tau_t$ . The relaxation time anisotropy will be characterized by the coefficient

$$k_\tau = \frac{\tau_e}{\tau_l}.$$

Recent research of the anisotropy of PbSb<sub>2</sub>Te<sub>4</sub> crystal reflection spectra, doped by Cu (Nemov et al. 2020) in the plasma reflection area, allows us to estimate the relaxation time anisotropy. The fact is that the experimental IR reflection spectra are well described in the framework of Drude-Lorentz model (Nemov et al. 2016; 2020) with the help of the dielectric function containing the parameter attenuation (damping) of the plasma oscillations  $\gamma$ , which is equal to  $\gamma = 1/\tau$ .

From the data (Nemov et al. 2020) we get:

$$k_{\tau} = \frac{\tau_e}{\tau_l} = \frac{\gamma_l}{\gamma_l} \approx \frac{44}{94} \approx 0.47 .$$

The received value of  $k_{\tau}$  indicates a strong anisotropy of hole scattering compared to other semiconductors. The frequency of plasma oscillations  $\omega_{pl}$  is determined by the formula:

$$\omega_{pl}^2 = \frac{4\pi pl^2}{\epsilon_{\infty} m^*} ,$$

where  $\epsilon_{\infty}$  is a high-frequency dielectric constant.

That is why the ratio of squares of the frequency of plasma oscillations at two orientations of light wave electrical vector  $\vec{E}$  along the axis  $\bar{3}$  and the plane cleavage make it possible to evaluate the anisotropy coefficient of the effective conductivity mass of  $k_m$ .

$$k_m = \left( \frac{\omega_l}{\omega_l} \right)_{pl}^2 \approx \left( \frac{0.52}{0.40} \right)^2 = 1.7 .$$

The received value confirms the elongated form of Fermi surface along the symmetry axis 3. The ratio of conductors in the chip plane  $\sigma_t$  to the conductivity  $\sigma_l$  along the axis 3 is:

$$\frac{\sigma_t}{\sigma_l} = \frac{\tau_l}{\tau_l} \times \frac{m_l}{m_{\tau}} = \frac{k_l}{k} . \tag{3}$$

Substituting certain values of the anisotropy coefficients  $k_m$  and  $k_{\tau}$  will get:

$$\frac{\sigma_t}{\sigma_l} \approx \frac{1.7}{0.47} = 3.6 ,$$

that is satisfactorily conforms with the data of electrical measuring.

As it was mentioned earlier, the studied crystals are not perfect. There are inclusions of the second phase of different composition and crystal lattice distortion. This circumstance explains some features of  $PbSb_2Te_4$  crystal reflection spectra, that was impossible to describe with the help of the complex dielectric function  $\epsilon(\nu)$  within the framework of Drude-Lorenz models. These include the existence of the inflection point on the dependence  $R(\nu)$  in the edge of plasma reflection area and the second small minimum in the area of  $2300 \text{ cm}^{-1}$  (see Fig. 3).

### Conclusion

So, as a result of X-ray studies of  $PbSb_2Te_4$  crystals and the analysis of the previously obtained experimental data on kinetic phenomena and IR reflections, the clarified valence zone structure and its parameters (effective weights of light and heavy holes, the temperature dependence of the energy gap between  $\Delta E_v(T)$  zones) were clarified.

We have also made the estimates of the anisotropy of effective mass of holes and relaxation time, indicating their strong anisotropy.

### Conflict of Interest

The authors declare that there is no conflict of interest, either existing or potential.

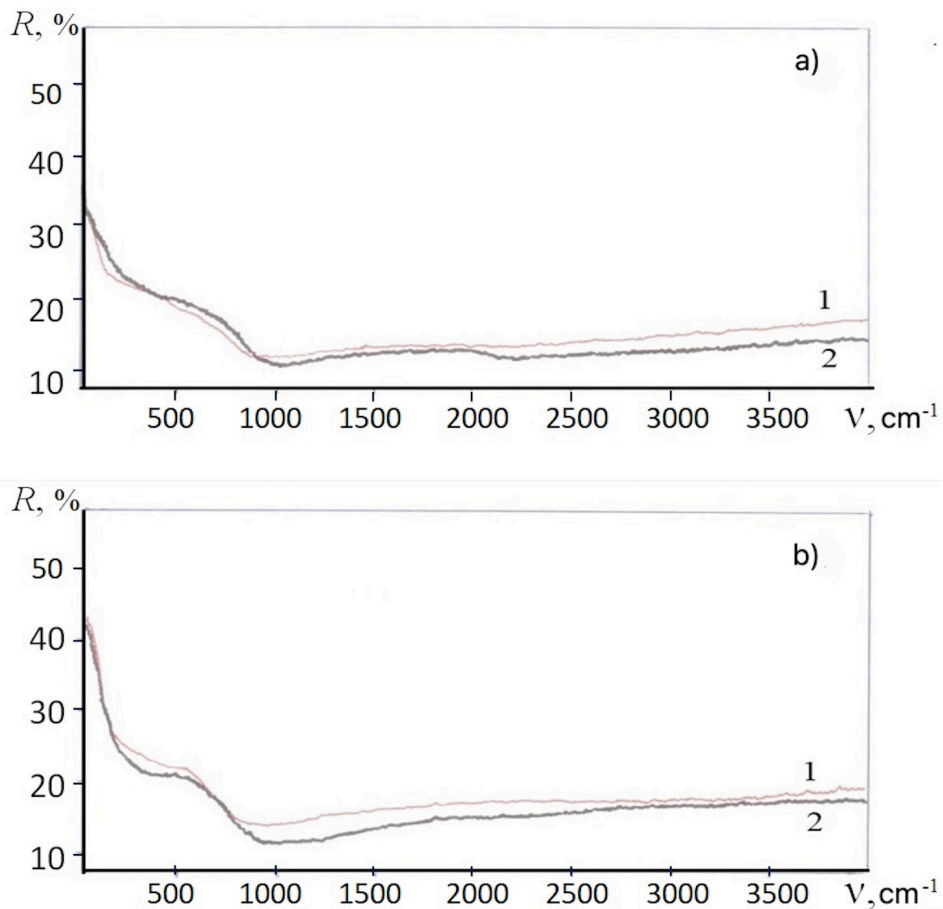


Fig. 3. Reflection spectra from the crystal chip  $\text{PbSb}_2\text{Te}_4$  (a) and  $\text{PbSb}_2\text{Te}_4:\text{Cu}$  (b): 1 –  $T = 300$  K; 2 –  $T = 77$  K

## References

- Goltsman, B. M., Kudinov, V. A., Smirnov, I. A. (1972) *Poluprovodnikovye termoelektricheskie materialy na osnove  $\text{Bi}_2\text{Te}_3$*  [Semiconductor thermoelectric materials based on  $\text{Bi}_2\text{Te}_3$ ]. Moscow: Nauka Publ., 320 p. (In Russian)
- Nemov, S. A., Blagikh, N. M., Dzhafarov, M. B. (2014) Effect of interband scattering on transport phenomena in p- $\text{PbSb}_2\text{Te}_4$ . *Semiconductors*, 48 (8), 999–1005. <https://doi.org/10.1134/S1063782614080193> (In English)
- Nemov, S. A., Blagikh, N. M., Shelimova, L. E. (2013) Features of the energy spectrum and hole-scattering mechanisms in  $\text{PbSb}_2\text{Te}_4$ . *Semiconductors*, 47 (1), 16–21. <https://doi.org/10.1134/S106378261301017X> (In English)
- Nemov, S. A., Ulashkevich, Yu. V., Pogumirsky, M. V., Stepanova, O. S. (2020) Reflection from the Side Face of a  $\text{PbSb}_2\text{Te}_4$  Crystal. *Semiconductors*, 54 (3), 282–284. <https://doi.org/10.1134/S1063782620030161> (In English)
- Nemov, S. A., Ulashkevich, Yu. V., Povolotskii, A. V., Khlamov, I. I. (2016) Reflectance of a  $\text{PbSb}_2\text{Te}_4$  crystal in a wide spectral range. *Semiconductors*, 50 (10), 1322–1326. <https://doi.org/10.1134/S1063782616100183> (In English)
- Shelimova, L. E., Karpinskii, O. G., Svechnikova, T. E. et al. (2004) Synthesis and structure of layered compounds in the  $\text{PbTe}-\text{Bi}_2\text{Te}_3$  and  $\text{PbTe}-\text{Sb}_2\text{Te}_3$  systems. *Inorganic Materials*, 40 (12), 1264–1270. <https://doi.org/10.1007/s10789-005-0007-2> (In English)
- Shelimova, L. E., Svechnikova, T. E., Konstantinov, P. P. et al. (2007) Anisotropic thermoelectric properties of the layered compounds  $\text{PbSb}_2\text{Te}_4$  and  $\text{PbBi}_4\text{Te}_7$ . *Inorganic Materials*, 43 (2), 125–131. <https://doi.org/10.1134/S0020168507020057> (In English)
- Zhitinskaya, M. K., Nemov, S. A., Shelimova, L. E. et al. (2008) Thermopower anisotropy in the layered compound  $\text{PbSb}_2\text{Te}_4$ . *Physics of the Solid State*, 50 (1), 6–8. <https://doi.org/10.1134/S1063783408010022> (In English)